Stem Cell Reports
Article

ISSCR

OPEN ACCESS

ERK5 promotes autocrine expression to sustain mitogenic balance for cell fate specification in human pluripotent stem cells

Chengcheng Song,[1,2,7] Zhaoying Zhang,[1,2,7] Dongliang Leng,[2] Ziqing He,[1,2] Xuepeng Wang,[3,4] Weiwei Liu,[1,2,5] Wensheng Zhang,[4] Qiang Wu,[3] Qi Zhao,[1,2] and Guokai Chen[1,2,6,8,*]

[1]Centre of Reproduction, Development and Aging, Faculty of Health Sciences, University of Macau, Taipa, Macau, China
[2]Faculty of Health Sciences, University of Macau, Taipa, Macau, China
[3]The State Key Laboratory of Quality Research in Chinese Medicine, Macau University of Science and Technology, Taipa, Macau, China
[4]CAM-SU Genomic Resource Center, Soochow University, Suzhou, Jiangsu, China
[5]Biological Imaging and Stem Cell Core Facility, Faculty of Health Sciences, University of Macau, Taipa, Macau, China
[6]Zhuhai UM Science & Technology Research Institute, Zhuhai, China
[7]These authors contributed equally
[8]Lead contact
*Correspondence: guokaichen@um.edu.mo
https://doi.org/10.1016/j.stemcr.2024.07.007

SUMMARY

The homeostasis of human pluripotent stem cells (hPSCs) requires the signaling balance of extracellular factors. Exogenous regulators from cell culture medium have been widely reported, but little attention has been paid to the autocrine factor from hPSCs themselves. In this report, we demonstrate that extracellular signal-related kinase 5 (ERK5) regulates endogenous autocrine factors essential for pluripotency and differentiation. ERK5 inhibition leads to erroneous cell fate specification in all lineages even under lineage-specific induction. hPSCs can self-renew under ERK5 inhibition in the presence of fibroblast growth factor 2 (FGF2) and transforming growth factor β (TGF-β), although *NANOG* expression is partially suppressed. Further analysis demonstrates that ERK5 promotes the expression of autocrine factors such as *NODAL*, *FGF8*, and *WNT3*. The addition of NODAL protein rescues *NANOG* expression and differentiation phenotypes under ERK5 inhibition. We demonstrate that constitutively active ERK5 pathway allows self-renewal even without essential growth factors FGF2 and TGF-β. This study highlights the essential contribution of autocrine pathways to proper maintenance and differentiation.

INTRODUCTION

Human pluripotent stem cells (hPSCs) have great potentials in basic research and regenerative medicine (Thomson et al., 1998; Takahashi and Yamanaka 2006; Yu et al., 2007). The decision of self-renewal or differentiation is often influenced by extracellular stimuli from their microenvironment that includes both exogenous factors in cell culture medium and endogenous autocrine factors from hPSCs themselves. However, much is unknown whether and how endogenous autocrine factors could contribute to these decision processes.

hPSCs resemble postimplant epiblast at primed state. Distinct mitogenic regulation is required for hPSC pluripotency and differentiation. Fibroblast growth factor 2 (FGF2), transforming growth factor β (TGF-β), and insulin in medium are sufficient for self-renewal by activating ERK1/2, SMAD2/3, and IGFR/PI3K/AKT pathways, while the lack of aforementioned stimuli leads to the exit of self-renewal, or even cell death (Chen et al., 2011; Godoy-Parejo et al., 2019; Ren et al., 2020; Zhou et al., 2022). In differentiation, the activation of bone morphogenetic protein (BMP)/FGF or WNT pathway promotes mesoderm differentiation (Lindsley et al., 2006; Bernardo et al., 2011; Greber 2011; Yu et al., 2011; Song et al., 2019); the inhibition of TGF-β/NODAL/Activin pathways induces ectoderm fate (Chambers et al., 2009; Wattanapanitch et al., 2014; Li et al., 2015; Madhu et al., 2016; Thakurela et al., 2016; Zhong et al., 2020); and BMP activation and TGF-β/NODAL/Activin/FGF inhibition together promote extraembryonic lineage (Xu et al., 2002; Zhang et al., 2008; Madhu et al., 2016). While those exogenous growth factors in medium are the main focus in cell fate determination, little is known about the role of hPSCs themselves in remodeling their own microenvironment. In this context, we ask a question, "Are hPSCs an active player in fate determination, or just a passive participant under exogenous signaling induction?".

Extracellular signal-regulated kinase 5 (ERK5, MAPK7, and big MAP kinase 1) is a unique member in the family of mitogen-activated protein kinases (MAPKs), because it contains not only a kinase domain but also a unique transcription activation domain (Kato et al., 1997; English et al., 1998; Drew et al., 2012; Nithianandarajah-Jones et al., 2012; Stecca and Rovida 2019; Paudel et al., 2021). After the phosphorylation by MEK5, ERK5 translocates to nucleus to regulate signal transduction and transcription. ERK5 is essential for mammalian embryogenesis. In mouse model, ERK5 knockout embryos can develop beyond gastrulation, but defective in placenta and cardiovascular development around embryonic days 9.5–10.5 with embryonic lethality (Yan et al., 2003). It suggests that

pluripotency can exist in ERK5 knockout blastocyst, but cell fate determination becomes defective *in vivo*. More ERK5 studies have been reported on mouse embryonic stem cells (mESCs) at naive state that resemble the inner cell mass in pre-implanted blastocyte. ERK5 and MEK5 inhibitors, such as XMD892, suppress the expression of pluripotency markers *Nanog* and *Rex1* in mESCs and induce naive-primed pluripotency transition and cardiac differentiation (Williams et al., 2016). The MEK5-ERK5 pathway induces *Klf2* to promote the expression of the mESC rejuvenation factor ZSCAN4 expression in the early embryonic 2-cell stage (Sunadome et al., 2011; Morikawa et al., 2016; Brown et al., 2021). However, it is unclear how ERK5 downstream effectors regulate pluripotency and cell fate determination in mESCs at naive state.

Because of ERK5's critical roles in embryogenesis, we investigate how ERK5 regulates primed pluripotency and differentiation in hPSCs. We hope to reveal the molecular mechanism of ERK5, so we could modulate hPSC more effectively for stem cell applications. In this study, we show that ERK5 is a master regulator for cell fate specification through endogenous autocrine pathways.

RESULTS

ERK5 is crucial for proper cell fate specification in hPSCs

In order to understand ERK5's function in hPSCs at the primed stage, we first examined its impact on spontaneous differentiation in neutral condition E6 medium without FGF2 and TGF-β (Zhong et al., 2020; Xu et al., 2021; Deng et al., 2022). Four days into spontaneous differentiation, most cells still aggregated together in colonies in E6 medium. However, colonies disintegrated with more cellular migration in the presence of ERK5 inhibitor XMD892 (XMD) (Figure 1A). Quantitative reverse-transcription PCR (RT-qPCR) analysis showed that XMD was more potent than E6 condition in suppressing the expression of pluripotency markers *NANOG* and *POU5F1* (Figure 1B). Although XMD induces mESCs into cardiomyocytes (Williams et al., 2016), human ESCs (hESCs) were not induced to cardiac fate after extended ERK5 inhibition by XMD (Figure S1A). These data suggested that ERK5 was beneficial to primed pluripotency of hPSCs in neutral condition, and hPSCs responded differently to ERK5 inhibition in comparison to mESCs.

Further analysis demonstrated that XMD in E6 medium suppressed mesoderm (*TBXT*(*Brachyury*) and *MIXL1*) and endoderm (*SOX17* and *FOXA2*) expression but promoted ectoderm (*PAX6* and *PAX3*) expression when compared with E6 medium alone (Figure 1C). The impact of ERK5 inhibition on neural expression was comparable to conventional neural induction through TGF-β/BMP dual inhibition by SB431542 and LDN193189 (SB + LDN) (Figure 1D). This result was confirmed by flow cytometry and immunostaining of PAX6 (Figures S1B and S1C). ERK5 inhibition-induced neural differentiation was also observed in H9 hESCs and NL4 human induced pluripotent stem cells (hiPSCs) (Figure S1D). We also showed that ERK5 inhibition and SB + LDN treatment had no synergistic effect on neural differentiation (Figure S1E).

We then investigated the impact of ERK5 inhibition on primitive streak induction with BMP4 in E8 medium containing FGF2 that later could give rise to mesoderm and endoderm lineages. XMD significantly reduced primitive streak markers *TBXT* (*Brachyury*) and *MIXL1* expression according to RT-qPCR analysis (Figure 1E). This finding was consistent with flow cytometry and immunostaining results (Figures S1F and S1G). We also demonstrated that ERK5 inhibition had similar impact on H9 hESCs and NL4 hiPSCs as well (Figure S1H). These results showed that ERK5 was essential for primitive streak induction.

We further analyzed ERK5's regulation in extraembryonic differentiation induced by BMP4 in the absence of FGF2 (Xu et al., 2002; Yu et al., 2011). We showed that ERK5 inhibitor significantly elevated the expression of extraembryonic markers such as *CGA* and *CGB*, even in the presence of FGF2 (Figure 1F). It suggests that ERK5 inhibition promoted extraembryonic differentiation induced by BMP4.

Another ERK5 inhibitor AX15836 (AX) was also used for cell lineage differentiation; the results showed that AX did not influence pluripotency maintenance but significantly promoted ectoderm fate and suppressed mesoderm differentiation (Figures S2A–S2C). These data demonstrated that AX15836's impact on hESCs was consistent with XMD892. We then validated ERK5 inhibitor's impact on cell fate determination with ERK5 knockdown cell line. *ERK5* (*MAPK7*) gene was knocked down by short hairpin RNA, and normal cellular morphology was observed in knockdown cell line (Figures S2D and S2E) in E8 medium. In E6 condition, ERK5 knockdown (sh*MAPK7*) led to ectoderm expression (Figure S2F) and suppressed primitive streak differentiation (Figure S2G). These results were consistent with the findings in inhibitor treatment on differentiation. Because ERK5 affected differentiation in all lineages, it suggests that ERK5 was involved in multiple pathways in cell fate determination. In order to study immediate effects, we used the inhibitor XMD to study ERK5 functions in this study.

hPSC pluripotency is maintained under ERK5 inhibition

Considering that ERK5 inhibition induces ectoderm differentiation in spontaneous differentiation, we examined

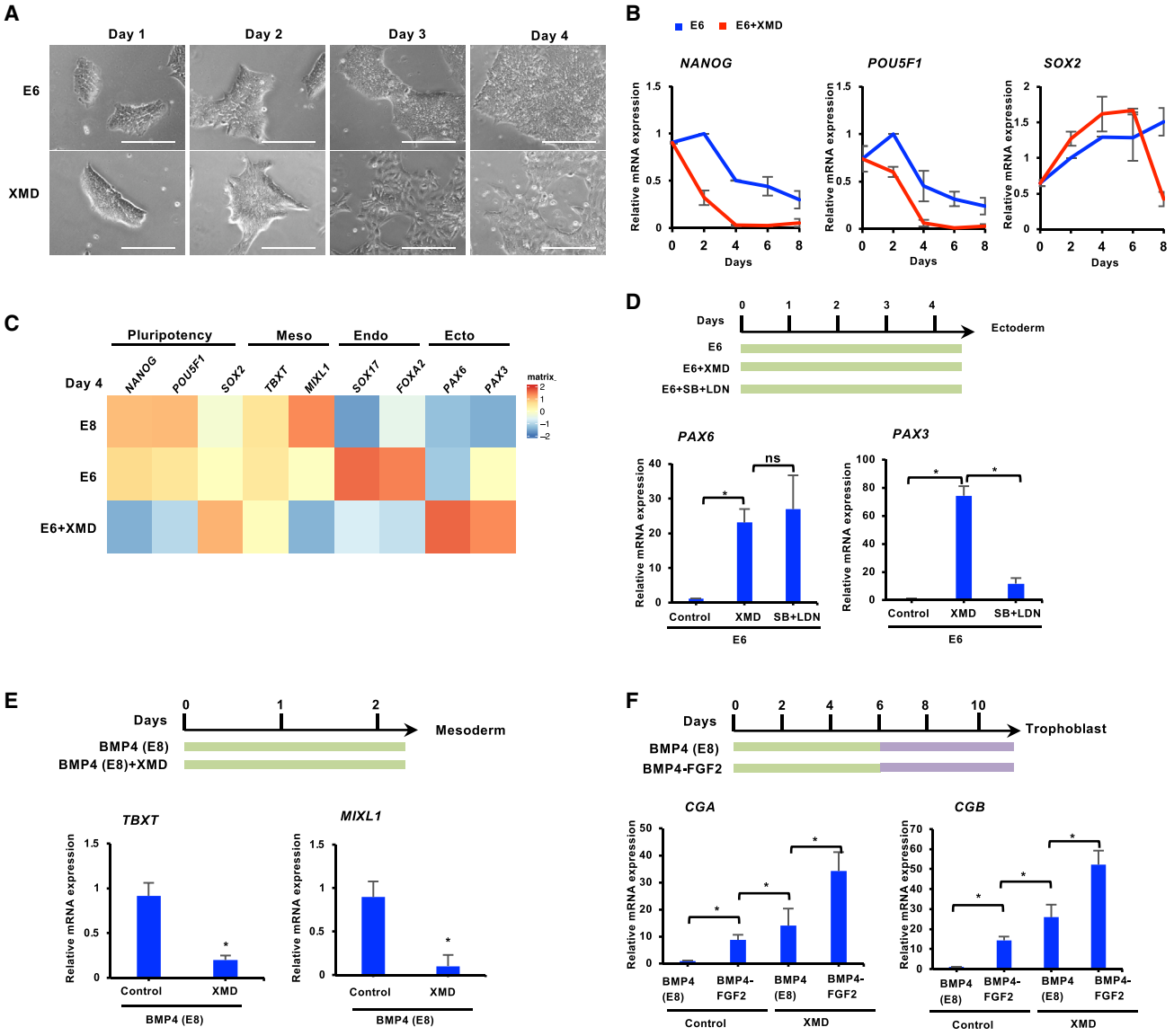

Figure 1. ERK5 is crucial for proper cell fate specification in hESCs

(A) Cell morphology of H1 ESCs cultured in spontaneous differentiation condition (E6 medium) with or without XMD (1 μM) from day 1 to day 4. Scale bar, 200 μm.

(B) RT-qPCR of pluripotency marker genes after H1 cells cultured in E6 medium with or without XMD from day 1 to day 8. NANOG, POU5F1, and SOX2 were used as pluripotency markers ($n = 3$).

(C) RT-qPCR analysis of lineage marker genes after H1 cells cultured in E6 medium with or without XMD for 4 days. TBXT and MIXL1 were used as mesoderm (Meso) markers, SOX17 and FOXA2 were used as endoderm (Endo) markers, and PAX6 and PAX3 were used as ectoderm (Ecto) markers ($n = 3$).

(D) Effect of ERK5 inhibition on ectoderm differentiation. H1 cells were induced toward ectodermal cell fate in E6 medium for 4 days with or without XMD before sample collection for RT-qPCR. SB431542 (10 μM) + LDN193189 (100 nM) were added ($n = 3$, $^*p < 0.05$. ns, not significant).

(E) Effect of ERK5 inhibition on mesoderm differentiation. H1 cells were induced toward mesodermal cell fate in BMP4 (20 ng/mL) with or without XMD for 2 days before sample collection for RT-qPCR ($n = 3$, $^*p < 0.05$).

(F) Effect of ERK5 inhibition on trophoblast differentiation. H1 cells were induced toward extra-embryonic cell fate in BMP4 (20 ng/mL) condition withdrawal FGF2 or not for 6 days with or without XMD, then continually cultured in E6 condition for 4 days before sample collection for RT-qPCR. CGA and CGB were used as trophoblast markers ($n = 3$, $^*p < 0.05$).

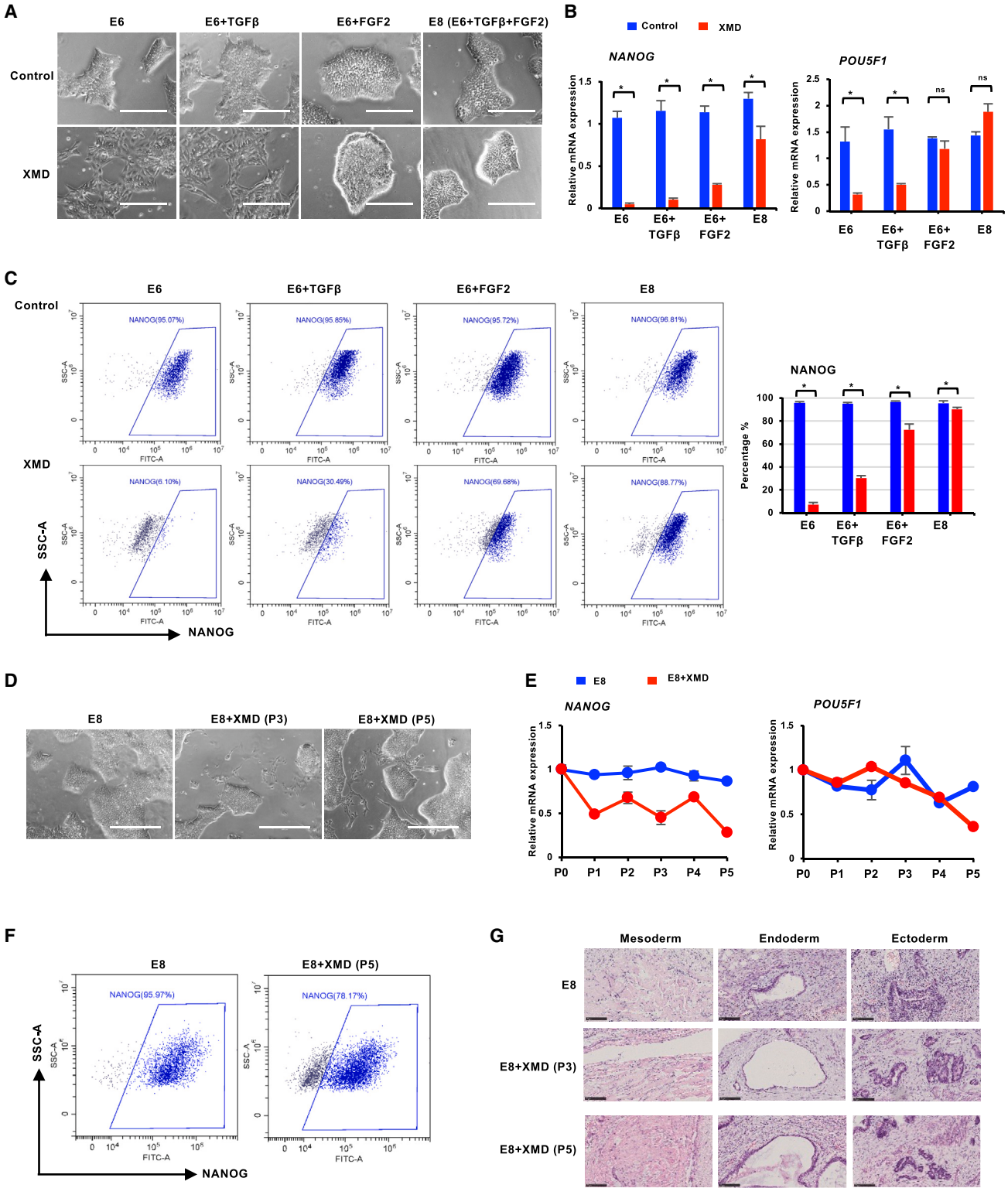

(legend on next page)

how pluripotency could be affected when FGF2 and TGF-β were provided. While ERK5 inhibitor induced cell migration in E6 medium after 3 days, the phenotype was suppressed by FGF2, but not by TGF-β. In regular E8 medium with TGF-β and FGF2, ERK5 inhibitor did not induce cell migration, and the tight colony morphology was maintained (Figure 2A). FGF2 also partially rescued the expression of *NANOG* and *POU5F1* in E6 condition (Figure 2B). These data suggested that ERK5 inhibition might lead to endogenous FGF signaling deficiency, which could be rescued by exogenous FGF2.

Although FGF2 could partially rescue stem cell phenotype under ERK5 inhibition, the mRNA expression levels of pluripotency markers were still repressed by ERK5 inhibition even in E8 maintenance medium (Figure 2B). However, more than 90% of cells were still positive in NANOG expression by flow cytometry after being cultured in E8 with ERK5 inhibition in 2 days (Figure 2C). However, TGF-β alone could not sustain *NANOG* expression. ERK5 knockdown cell line also had lower *NANOG* mRNA expression, but most cells demonstrate positive NANOG expression (Figure S2H).

Furthermore, we examined the impact of ERK5 inhibition in extended culture for more than 5 passages in E8 medium. We showed that hESCs could be expanded normally under ERK5 inhibition (Figure 2D). Although regular colony morphology was observed after several passages, some individual differentiated cells emerged in cell culture after 3 passages. RT-qPCR showed that *NANOG* mRNA expression was constantly lower under ERK5 inhibition than control, but its expression level was maintained after initial decrease. Flow cytometry analysis showed that the majority of cells were still NANOG positive even after several passages (Figures 2E and 2F). This result was consistent with the fact that ERK5 knockdown line could be established in E8 medium (Figure S2D). These data indicated that pluripotency might be maintained under ERK5 inhibition because pluripotency marker expression was not turned off totally.

In order to examine the pluripotency of hPSCs after ERK5 inhibition, we treated H1 hESC with XMD after 5 passages, and then injected the cells into nude mouse for teratoma assay. Teratomas were formed after several weeks, and all three embryonic lineages were observed (Figure 2G). Teratomas were also successfully obtained from H9 hESCs and NL4 hiPSCs after XMD treatment for 5 passages (Figure S2I). These data suggested that pluripotency was maintained under ERK5 inhibition, even though *NANOG* mRNA level was partially suppressed.

ERK5 regulation on transcriptome in hPSCs

In order to understand ERK5 regulation in hPSCs, we examined transcriptome profile under ERK5 inhibition in E8 condition. RNA sequencing (RNA-seq) analysis was conducted on hESCs treated by XMD in a time course (12, 24, and 48 h). XMD-treated samples were clustered together in comparison to E8 control (Figures S3A and S3B). We further analyzed genes significantly affected by ERK5 inhibition for 12, 24, and 48 h. According to Kyoto Encyclopedia of Genes and Genomes (KEGG) analysis, XMD modulated gene expression in a time-dependent manner (Figures S3C and S3D). Especially, XMD suppressed gene expression in diverse signaling pathways related to pluripotency such as TGF-β pathway within 12 h (Figure S3D). We further conducted gene ontology (GO)-term and KEGG analysis of significantly affected genes by 48 h XMD treatment. The results showed that XMD elevated gene expression in metabolism related to sulfur, fatty acids, and amino acids. XMD-suppressed signaling pathways regulated transmembrane receptor protein serine/threonine kinase and SMAD protein phosphorylation and downregulated gene expression in signaling pathways related to pluripotency in stem cells, cell adhesion, and ligand-receptor interaction (Figure 3A).

Due to ERK5's impact on *NANOG* expression, we were particularly interested in the signaling pathways related to pluripotency. Volcano plot showed that a set of

Figure 2. hPSC pluripotency is maintained under ERK5 inhibition

(A) Cell morphology of H1 cells cultured in multiple conditions with or without XMD for 4 days. E6, E6 + FGF2, E6 + TGF-β, and E8 (E6 + FGF2 + TGF-β) conditions were conducted. Scale bar, 200 μm.

(B) RT-qPCR analysis of pluripotency markers expression after H1 cells cultured in multiple conditions as (A) with or without XMD for 3 days ($n = 3$, $^*p < 0.05$. ns, not significant).

(C) Fluorescence-activated cell sorting (FACS) analysis of NANOG expression on day 3 treated with multiple conditions as (A) with or without XMD in H1 cells. Left, representative image of histogram. Right, bar graph showing mean ± SD of three independent experiments ($n = 3$, $^*p < 0.05$).

(D) Cell morphology of H1 cells cultured in E8 with or without XMD after 3 passages (P3) and 5 passages (P5). Scale bar, 400 μm.

(E) RT-qPCR analysis of pluripotency markers expression during H1 cells cultured in E8 with or without XMD after 5 passages ($n = 3$).

(F) FACS analysis of NANOG expression during H1 cells cultured in E8 with or without XMD after 5 passages ($n = 3$).

(G) Teratoma analysis of H1 cells cultured in E8 with XMD after 3 passages (P3) and 5 passages (P5). Lineage tissues of mesoderm/endoderm/ectoderm were displayed. Scale bar, 100 μm.

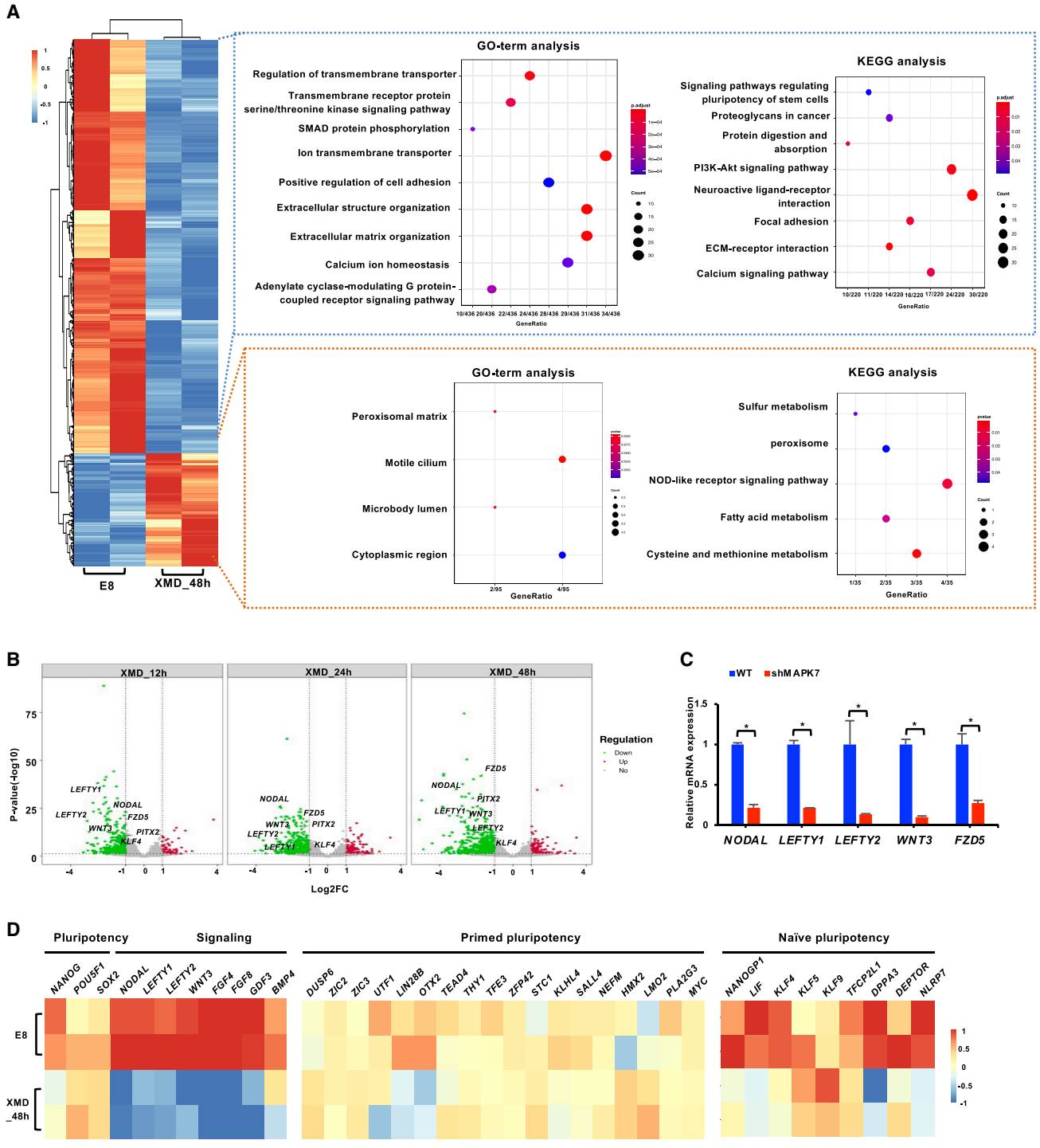

Figure 3. ERK5 regulation on transcriptome in hPSCs

(A) Differentially expressed genes (DEGs) profile of RNA-seq data after XMD treated for 48 h in H1 cells. XMD-induced upregulated genes and downregulated genes were analyzed for gene ontology (GO) and KEGG enrichment separately.

(B) Volcano plot of DEGs in item of signaling pathways regulating pluripotency of stem cells from GO analysis of downregulated genes by XMD treatment as (A) in H1 cells. XMD treated for 12/24/48 h.

(legend continued on next page)

pluripotency-related genes in KEGG analysis were all downregulated within just 12 h of XMD treatment (Figure 3B). Besides *NANOG* and *KLF4*, many genes were all directly involved in growth factor signaling pathways. For example, *NODAL*, *LEFTY1*, *and LEFTY2* belong to the TGF-β/NODAL pathway, while *WNT3* and *FZD5* are involved in the WNT pathway. It was confirmed that *ERK5* knockdown (sh*MAPK7*) also significantly decreased the expression of those genes (Figure 3C). We further showed that more genes in mitogen-related signaling pathways were downregulated by ERK5 inhibition (Figures S3E–S3H). *FGF4*, *FGF8*, *GDF3*, *and BMP4* were a few common growth factors suppressed by ERK5 inhibition (Figure 3D). These data suggested that ERK5 could be a master regulator of endogenous growth factor expression.

Pluripotency gene analysis showed that ERK5 inhibition suppressed *NANOG* expression, but did not affect *OCT4* (*POU5F1*) and *SOX2* expression (Figure 3D). These data were consistent with RT-qPCR results (Figure 2). Most primed pluripotency genes did not show significant changes under ERK5 inhibition, but some naive pluripotency genes were partially suppressed, including *KLF4*, *TFCP2L1*, *DPPA3*, *DEPTOR*, *NLRP7*, *and LIF* (Figure 3D). These data supported the notion that the primed pluripotency could be maintained under ERK5 inhibition, although some stage-specific genes were suppressed.

We also conducted epigenetic analysis with histone modification chromatin immunoprecipitation sequencing (ChIP-seq) (H3K27ac and H3K4me3) to evaluate the impact of ERK5 inhibition. H3K27ac and H3K4me3 are well known as activation modification (Pan et al., 2007; Creyghton et al., 2010; Hawkins et al., 2010; Battle et al., 2019). We showed that ERK5 inhibition did not significantly influence genome-wide profiles of both H3K27ac and H3K4me3 modification (Figure S3I). Furthermore, we compared the differentially expressed genes from H3K27ac and H3K4me3 ChIP-seq. The results showed that ERK5 inhibition significantly suppressed H3K27ac modification on *KDR* and *NODAL*, while the inhibition significantly promoted H3K27ac and H3K4me3 modification on *SFRP1* expression to suppress WNT pathway (Uren et al., 2000; Liang et al., 2019) (Figures S3J–S3L). ERK5 inhibition significantly suppressed *NODAL* expression with decreased H3K27ac and H3K4me modification; however, ERK5 inhibition did not affect the epigenetic profiles of *NANOG*, *FZD5*, and *FGF4* (Figure S3L). These results indicated that ERK5 inhibition on NODAL expression might be associated with epigenetic regulation.

NODAL can rescue cell fate specification under ERK5 inhibition

Transcriptome data showed that ERK5 inhibition suppressed a set of growth factors associated with pluripotency (Figure 3), so we examined whether the growth factor function was associated with ERK5's functions in hPSCs. In order to understand ERK5's regulation, we first confirmed that ERK5 inhibition indeed suppressed gene expression in TGF-β/NODAL and WNT pathways (Figures 4A and S4A). We then showed that ERK5 inhibition suppressed SMAD2 phosphorylation (Figures S4B and S4C), but the phenotype was rescued by the addition of recombinant NODAL (Figure 4B). These results suggested that ERK5 inhibition potentially affected maintenance and differentiation through the suppression of TGF-β/NODAL pathway.

We further showed that exogenous NODAL partially rescued the gene expression of *NANOG* under ERK5 inhibition in E8 medium (Figure 4C). NODAL also significantly promoted endogenous expression in *NODAL* itself and *WNT3*. Additionally, TGF-β also rescued *NANOG* expression under XMD treatment for multiple passages in E8 medium (Figures S4D–S4F). It suggested that NODAL could be a downstream endogenous effector of ERK5 in the maintenance of hPSC pluripotency.

We then inspected the impact of exogenous NODAL on cell fate determination under ERK5 inhibition. First, NODAL supplement significantly suppressed the neural expression of *PAX6* and *PAX3* induced by ERK5 inhibition in E6 medium (Figure 4D). Second, NODAL supplement also rescued *TBXT* and *MIXL1* expression during mesoderm differentiation under BMP4 induction (Figure 4E). Meanwhile, NODAL also promoted endogenous expression of *NODAL*, *WNT3*, *FZD5*, *LEFTY1*, *and LEFTY2 in both E6 condition and BMP4 condition* (Figure 4F). In contrast to NODAL, the addition of WNT3A did not promote mesoderm differentiation and did not promote the expression of *NODAL* and *WNT3* (Figure S4G). These data suggested that ERK5 probably influenced cell fate determination through NODAL.

We further examined whether NODAL could modulate mESCs under ERK5 inhibition. Similar to hPSCs, exogenous NODAL rescued pluripotency gene expression under ERK5 inhibition, such as *Nanog*, *Klf4*, *Esrrb*, and *Rex1* (Figure S4H).

Continuous ERK5 activation sustains pluripotency without common exogenous growth factor stimulation

Because ERK5 inhibition suppressed the endogenous expression of many growth factors related to pluripotency

(C) RT-qPCR analysis of genes expression related to TGF-β/NODAL and WNT pathways in shMAPK7 H1 cell line ($n = 3$, $^*p < 0.05$).
(D) Heatmap analysis of genes related to pluripotency, signaling pathways, primed pluripotency, and naive pluripotency after XMD treated for 48 h in H1 cells. *NODAL*, *LEFTY1*, and *LEFTY2* were used as markers of TGF-β/NODAL pathway, *WNT3* was used as marker of WNT pathway, *FGF4* and *FGF8* were used as markers of MAPKs pathway, and *BMP4* and *GDF3* were used as markers of BMPs pathway.

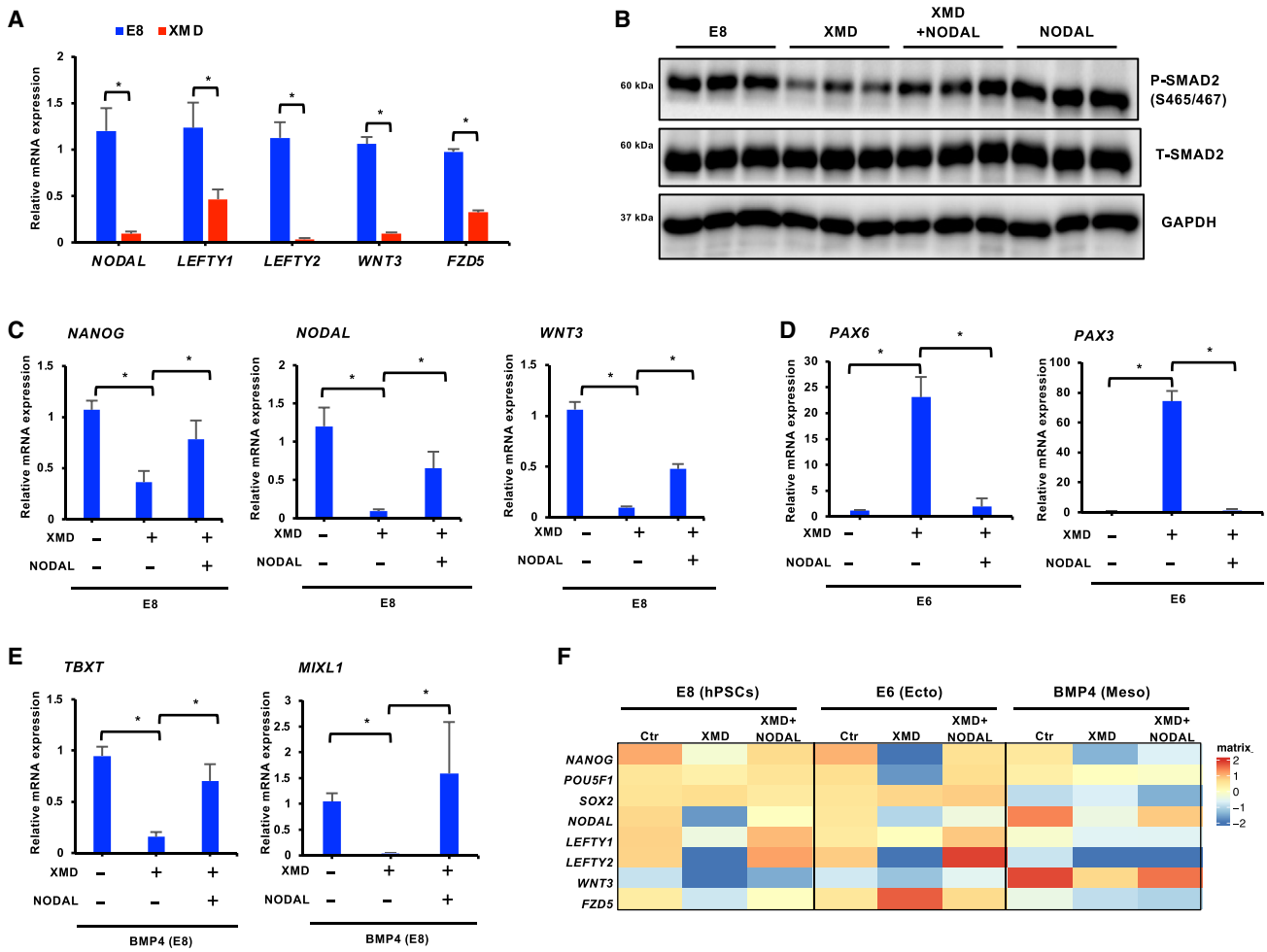

Figure 4. NODAL can rescue ERK5 inhibition-induced cell fate identity

(A) RT-qPCR analysis of gene expression related to TGF-β/NODAL pathway and WNT pathway of H1 cells treated with or without XMD for 2 days ($n = 3$, $^*p < 0.05$).

(B) Western blotting analysis of SMAD2 phosphorylation after XMD and NODAL treatment in H1 cells. H1 cells were subjected to treat for 24 h. XMD and NODAL (100 ng/mL) were added.

(C) RT-qPCR analysis of NODAL rescued gene expression, which was downregulated by XMD in E8 condition for 2 days in H1 cells ($n = 3$, $^*p < 0.05$. ns, not significant).

(D) RT-qPCR analysis of NODAL rescued ectoderm gene expression, which was upregulated by XMD in E6 condition for 4 days in H1 cells ($n = 3$, $^*p < 0.05$. ns, not significant).

(E) RT-qPCR analysis of NODAL rescued mesoderm gene expression, which was downregulated by XMD in BMP4 condition for 2 days in H1 cells ($n = 3$, $^*p < 0.05$. ns, not significant).

(F) RT-qPCR analysis of NODAL rescued gene expression related to TGF-β/NODAL pathway and WNT pathway in the condition of pluripotency maintenance (C), ectoderm (D), and mesoderm (E) differentiation in H1 cells ($n = 3$).

(Figure 3), we examined whether continuous ERK5 activation could affect the reliance on exogenous factors for pluripotency in hPSCs. A constitutively active ERK5 cell line (MEK5DD cell line) was generated from H1 hPSCs by overexpressing MEK5 with specific mutations (Ser311 to Asp, Ser315 to Asp, MEK5DD), which continuously activates ERK5 (Kato et al., 1997; English et al., 1999; Williams et al., 2016; Brown et al., 2021). When ERK5 was constitutively active, there were no significant morphological changes in E8 medium (Figures 5A, S5A, and S5B), and pluripotency gene expression was not significantly affected (Figures S5C and S5D). However, the expression of *NODAL*, *WNT3*, and *FGF8* was significantly increased (Figure 5B). We then showed that mesoderm induction by BMP4 was elevated in MEK5DD cell line (Figure S5E). These data suggested that ERK5 activation

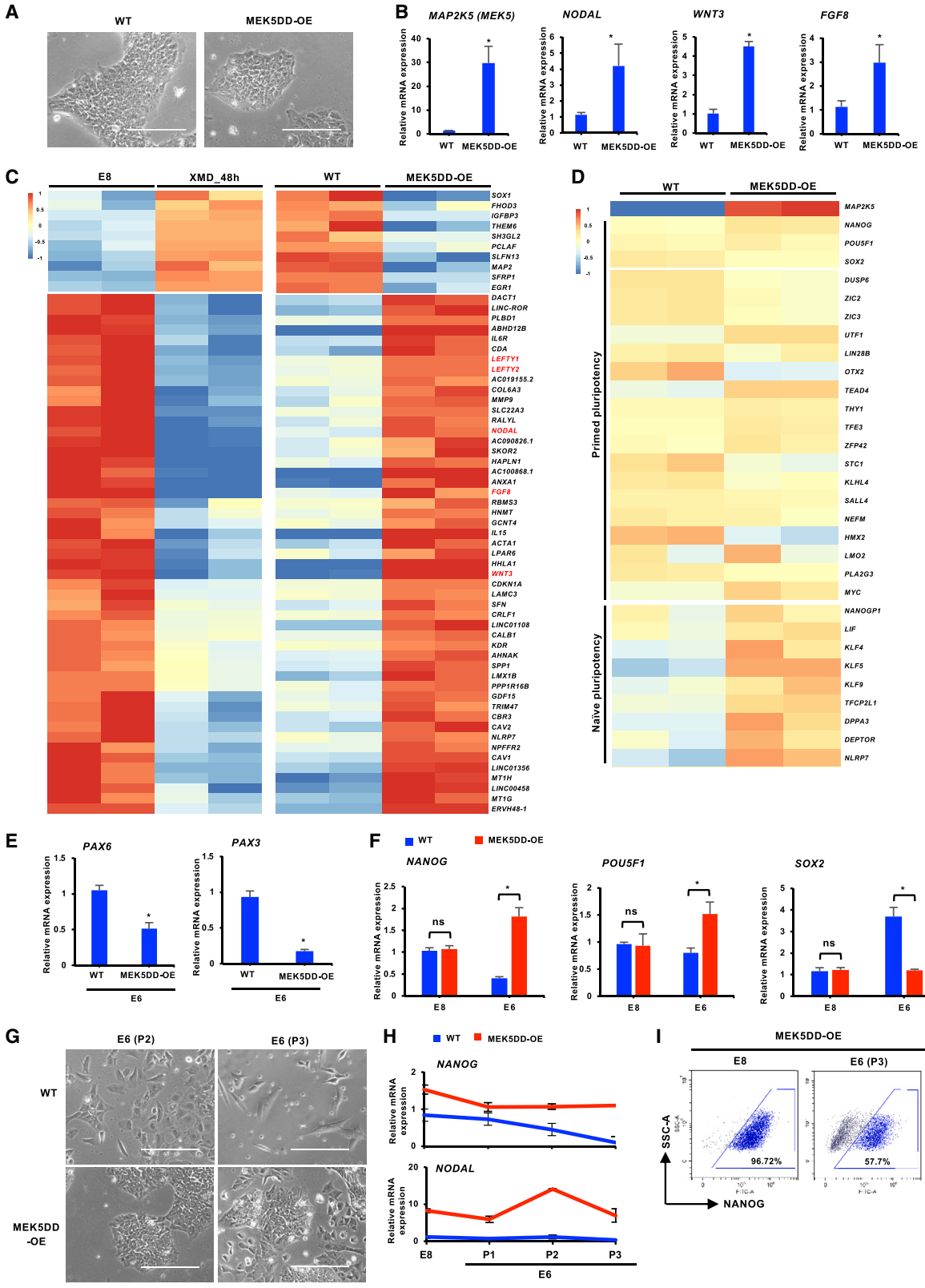

(legend on next page)

could regulate cell fate through endogenous NODAL expression.

We then conducted transcriptome analysis on MEK5DD cell line. GO-term and KEGG analysis showed that MEK5DD-downregulated genes were enriched in synapse organization and neurodevelopment, and MEK5DD-upregulated genes were enriched in SMAD protein signaling transduction and signaling regulation on pluripotency of stem cells (Figure S5F). We then focused on gene expression related to signaling pathways including TGF-β/NODAL, WNT, BMP, and FGF (Figures S5G–S5J). Constitutively active ERK5 elevated gene expression such as *NODAL*, *LEFTY1*, *LEFTY2*, *WNT3*, and *FGF8* expression, which were suppressed by ERK5 inhibition (Figure 5C). Meanwhile, ERK5 activation did not significantly affect the expression related to the primed state, but promoted some gene expression related to naive pluripotency (Figure 5D). These results were consistent with the study of ERK5 inhibition (Figure 3).

FGF2 and TGF-β are essential factors to maintain pluripotency in wild-type hPSCs. We showed that either TGF-β or FGF2 alone was sufficient to sustain *NANOG* and *POU5F1* expression in MEK5DD cell line, as well as regular stem cell morphology (Figures S6A–S6G). It suggests that ERK5 activation promoted pluripotency at sub-optimal conditions.

Because of ERK5's important role in pluripotency and cell fate determination, we then examined whether pluripotency could be maintained with constitutively active ERK5 in E6 medium without FGF2 and TGF-β. We found that ectoderm marker genes *PAX6* and *PAX3* were suppressed in MEK5DD cell line compared with wild-type cells (Figure 5E). Pluripotency genes *NANOG* and *POU5F1* were maintained in MEK5DD cell line after 3 days, although those genes' expression decreased more significantly in wild-type cells (Figure 5F). Furthermore, both cell lines were passaged in E6 condition for an extended period. Almost all wild-type cells differentiated after 2 passages in E6 condition. However, MEK5DD cell line maintained normal cell morphology after 2 passages, but differentiated cells emerged after 3 passages (Figure 5G). *NANOG* was upregulated in MEK5DD cell line after 3 passages in E6 medium (Figures 5H and 5I).

We recently showed that lysophosphatidic acid (LPA) was reported to activate the AMPK pathway and the ERK1/2 pathway (Xu et al., 2021). When LPA was applied to MEK5DD cell line, ERK5 activation helped maintain the expression of *NANOG* and *NODAL* in E6 medium for more than 5 passages (Figures S6H–S6I). These data suggested that MEK5DD cell line can help maintain pluripotency without FGF2 and TGF-β.

Endogenous NODAL expression as a biomarker in hPSCs

Transcriptional factors such as NANOG and KLF4 are common markers for people to describe the cellular status in pluripotent stem cells. In this study, we showed that growth factor expression such as NODAL could have profound impact on cell fate. We hypothesized that growth factor expression profile might be a useful biomarker in hPSC analysis. We compared transcriptomes of four common hPSC lines in the lab (H1, H9, NL1, and NL4). We showed that many ERK5-regulated growth factor genes were closely correlated with *NANOG* expression, including *NODAL*, *WNT3*, *FGF4*, *and GDF3* (Figure 6A). Meanwhile, those growth factors were highly correlated with *NODAL* expression as well ($R > 0.6$) (Figure 6B). These data suggested that a set of growth factors were expressed in a coordinated manner, likely through ERK5 pathway.

We further examined the endogenous growth factor gene expression in public database of 317 hiPSC lines from 101 individuals (Carcamo-Oriveet al. 2017) (Figure 6C). *NANOG* expression level did not clearly correlate with the expression level of those growth factors. However, ERK5-targeted genes *GDF3*, *WNT3*, *FGF4*, and *FGF8* closely correlated with *NODAL* (Figures 6D and S6J). Principal component analysis showed that 317 hiPSC lines were separated into two clusters based on the expression of those genes (Figures 6E and S6K). Furthermore, we processed uniform manifold approximation and projection (UMAP) analysis to detect variability in hiPSC lines induced by multiple sources mentioned in the reference. Clusters were

Figure 5. Continuous ERK5 activation sustains pluripotency without common growth factor stimulation

(A) Cell morphology of MEK5DD-OE H1 cell line cultured in E8 medium. Scale bar, 200 μm.

(B) RT-qPCR analysis of genes expression in MEK5DD-OE H1 cell line ($n = 3$, $^*p < 0.05$).

(C) Heatmap analysis of DEGs between MEK5DD-OE H1 cells and XMD-treated H1 cells.

(D) Heatmap analysis of genes related to primed pluripotency and naive pluripotency in MEK5DD-OE H1 cell line.

(E) RT-qPCR analysis of ectoderm genes expression in MEK5DD-OE H1 cell line cultured in E6 condition for 4 days ($n = 3$, $^*p < 0.05$).

(F) RT-qPCR analysis of pluripotency gene expression in MEK5DD-OE H1 cell line cultured in E8 and E6 conditions ($n = 3$, $^*p < 0.05$. ns, not significant).

(G) Cell morphology of MEK5DD-OE H1 cell line cultured in E6 medium after 3 passages (P3). Scale bar, 200 μm.

(H) RT-qPCR analysis of *NANOG* and *NODAL* genes expression in MEK5DD-OE H1 cell line cultured in E6 medium after 3 passages (P3) ($n = 3$).

(I) FACS analysis of NANOG expression in MEK5DD-OE H1 cell line cultured in E6 medium after 3 passages (P3).

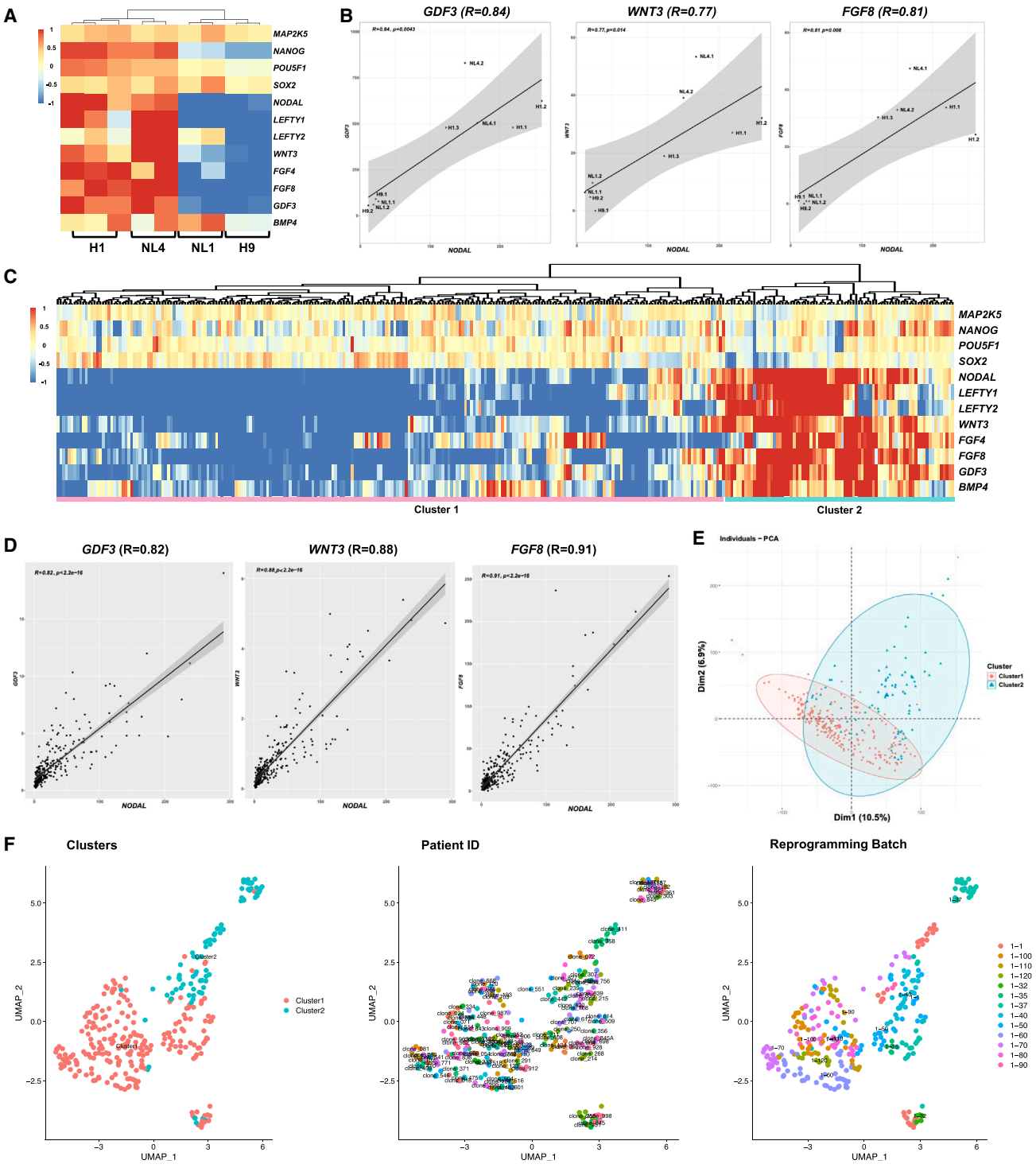

Figure 6. NODAL as a biomarker for autocrine expression in hPSCs

(A) Heatmap analysis of mitogen expression in 4 hPSC lines (H1, H9, NL1, and NL4 cell lines).

(B) Correlation analysis of gene expression of mitogens to *NODAL* expression in 4 hPSC lines (H1, H9, NL1, and NL4 cell lines).

(C) Heatmap analysis of gene expression of mitogens in hiPSC clones.

(D) Correlation analysis of gene expression of mitogens to *NODAL* expression in hiPSC clones.

(E) Principal component analysis (PCA) profile of hiPSC clones. Clusters of clones were displayed.

(F) UMAP profile in hiPSC clones. Clusters, patient ID, and reprogramming bath were analyzed.

separated in the UMAP, and patient ID and reprogramming batch showed the essential factors for variability in two clusters (Figure 6F). Other factors such as sex, source cell, batch, and reprogramming technicians did not contribute significantly to the growth factor differences (Figures S6L and S6M). These data suggested that the endogenous autocrine expression was regulated coordinately. This regulation is more related to the genetic characters of individuals and reprogramming batches, but not the sex, source cell, and technical variables (Rouhani et al., 2014; Burrows et al., 2016; Carcamo-Orive et al., 2022).

DISCUSSION

The balance of signal transduction is essential for the maintenance and cell fate determination of hPSCs. Despite the influence of exogenous growth factors from culture medium, hPSCs also generate endogenous factors as autocrine feedback to fine-tune cellular functions. When endogenous expression is comprised, it leads to erroneous cell fate determination. This study highlights hPSC autocrine as a potent target in stem cell applications.

ERK5 has a more complicated cellular function than other MAPKs with both kinase and transcriptional domains. ERK5 is involved in various processes, such as cell proliferation, tumor metastasis, metabolism, and stemness. ERK5 also plays roles in tumor microenvironment and angiogenesis. This study reveals ERK5 as a master regulator of numerous endogenous growth factors in many pathways, such as TGF-β/NODAL, BMP, WNT, and FGF. These diverse endogenous growth factors modulate different processes simultaneously through a single gene in ERK5. Constitutively, activation of ERK5 allows hPSCs to self-renew in suboptimal conditions even without both FGF2 and TGF-β, because endogenous growth factors are probably enough for pluripotency maintenance under ERK5 regulation. When ERK5 is suppressed in hPSCs, the lack of endogenous autocrine input leads to erroneous cell fate determination in all lineages. These findings help explain the abnormal development in different lineages and embryonic lethality in ERK5 knockout mice.

In order to maintain hPSCs, TGF-β or NODAL must be provided in culture medium. People usually consider that exogenous factors are all the cells need for regular hPSC phenotypes. However, we show that endogenous NODAL actually contributes significantly to cellular functions. When endogenous NODAL is suppressed by ERK5 inhibition, *NANOG* expression is repressed. Exogenous NODAL rescues not only NANOG expression but also other growth factors in WNT, TGF-β, and FGF pathways. The addition of NODAL also restores cell fate determination under ERK5 inhibition. A recent report demonstrates that *NODAL* knockout can be generated, but with deficiency in mesoderm differentiation, resembling a major phenotype under ERK5 inhibition (Liu et al., 2022). These facts make NODAL a chief effector of ERK5 to regulate hPSC function. It is also interesting to find that exogenous NODAL could rescue *Nanog* expression in mESCs. This demonstrates NODAL as a key regulator in different pluripotent stage in different species. It is consistent with the notion that TGF-β/NODAL superfamily is essential for the transcriptomic characteristics connecting to naive pluripotency state in hPSCs (Watanabe et al., 2022). More study is necessary to figure out how ERK5 specifically targets NODAL expression through epigenetic regulation. It would also be interesting to learn more about the functional difference among TGF-β/NODAL family members.

hPSCs can maintain pluripotency in a continuum of cellular states, while cell proliferation and metabolism are greatly changed (Cliffet al., 2017; Xu et al., 2021; Zhou et al., 2022). The expression level of NANOG is often considered as critical for pluripotency state. It is generally believed that naive state cells have higher *NANOG* expression, while the decrease of *NANOG* expression indicates the exit of self-renewal (Gu et al., 2016; Gatchalian et al., 2018; Pera and Rossant 2021). This study demonstrates that *NANOG* expression is associated with endogenous *NODAL* level. Even with lower *NANOG* under ERK5 inhibition, hPSCs can be expanded for multiple passages, while normal teratomas are formed, implying the maintenance of pluripotency. It suggests that partially NANOG suppression is not a sufficient evidence for the loss of pluripotency. Instead, it is necessary to examine pluripotency with more strict assays that involve extended culture and teratoma formation.

In summary, we demonstrate hPSCs as an active player in their cell fate determination through the endogenous autocrine growth factors. We also reveal ERK5 as a central regulator of endogenous growth factors. ERK5 and endogenous growth factors could serve as valuable targets to improve stem cell applications.

EXPERIMENTAL PROCEDURES

Key resources table

The key resources table is available in supplemental information.

Resource availability

Lead contact

Further information and requests for resources and reagents should be directed to the lead contact, G.C. (guokaichen@um.edu.mo).

Materials availability

This study did not generate new unique reagents.

Data and code availability

The bulk RNA-seq data and ChIP-seq data used in this article are deposited on NCBI. The accession numbers in this article are

GEO: GSE234058 and GEO: GSE247041. No new code was generated in this study.

Experimental model and subject details

hPSC culture

hPSC lines (H1, H9, and NL4) were maintained in E8 medium with Penicillin/Streptomycin as published before (Chen et al., 2011). E8 medium was home-made containing DMEM/F12 (Thermo), sodium selenite (Sigma), ascorbic acid trisodium (Sigma), transferrin (Sigma), TGF-β (PeproTech), FGF2 (home-made), and insulin. Cells were cultured on Matrigel (Corning)-coated plate. Cells were dissociated in DPBS-EDTA as published before (Beers et al., 2012). ROCK inhibitor Y27632 (DC chemicals) was used during cell passage. The use of hESCs and hiPSCs was approved by the institutional review board at the University of Macau.

mESC culture

mESC line (E14) was cultured on 0.1% gelatin-coated plate and was maintained in medium comprising DMEM (Thermo), LIF (Millipore), 10% FBS (Thermo), NEAA (Thermo), and 2-Mercaptoethanol (Sigma) as published before (Zhang et al., 2019). Medium was changed every 2 days, and cells were passaged every 3–4 days. During passage, cells were washed by PBS and then dissociated in TrypLE.

Differentiation of hESCs

Spontaneous differentiation. Spontaneous differentiations were induced for 4 days in E6 medium (DMEM/F12 with the addition of sodium selenite, ascorbic acid trisodium, transferrin, and insulin). 1 μM XMD892 (Selleck) was added for 4 days or not. Medium was changed every day. *NANOG*, *POU5F1*, and *SOX2* were used as pluripotency markers.

Ectoderm differentiation. Ectoderm differentiation was conducted for 4 days in E6 medium, supplied with 10 μM SB431542 (Selleck) and 100 nM LDN193189 (Selleck). 1 μM XMD892 was added for 4 days. Medium was changed every day. *PAX6* and *PAX3* were used as ectoderm markers.

Mesoderm differentiation. Mesoderm differentiation was conducted for 2 days in E8 medium supplied with 20 ng/mL BMP4 (R&D Systems). 1 μM XMD892 was added for 2 days. *TBXT* and *MIXL1* were used as mesoderm markers.

Extra-embryonic differentiation. Extra-embryonic differentiation was conducted for 10 days. *CGA* and *CGB* were used as extra-embryonic markers.

Day 1–6: E6 medium with TGF-β and 20 ng/mL BMP4 was added. 1 μM XMD892 was used. Medium was changed every day.

Day 7–10: E6 medium was conducted. Medium was changed every day.

RNA extraction and real-time qPCR. RNA was extracted after samples harvested in RNAiso Plus reagent (Takara). cDNA was synthesized in 10 μL system (500 ng RNA/sample) using High-capacity cDNA reverse transcription kit (Applied Biosystems). Real-time qPCR was conducted on Applied Biosystems QuanStudio 7 Flex Real-time PCR system (Lif technology) with SYBR Premix Ex TaqTM (Takara). Primers used for real-time qPCR were listed in the Table S1.

Western blotting. Samples were scraped in 2X Laemmli buffer. Protein level was detected by Protein concentration BCA protein assay kit (Thermo). Run gel SDS-PAGE gels under 100 V. Proteins were transferred to PVDF membranes. PVDF membrane was blocked in 2% BSA buffer in 1X TBST for 1 h. Primary antibody was cultured in 1% BSA 1X TBST overnight, and then washed in 1X TBST. HRP-secondary antibody was cultured in 1X TBST for 1–2 h, and then washed in 1X TBST. Proteins were exposed by SuperSignal West Pico PLUS Chemiluminescent Substrate kit (Thermo) or SuperSignal West Dura Extended Duration Substrate kit (Thermo).

Flow cytometry. Harvest sample by TrypLE for 5 min and neutralize by 5% FBS. Wash cells with 1 mL 1X PBS and spin down at 300 g for 5 min. Cells were fixed in 1% PFA for 10–15 min, and then washed in 1X PBS. Cells were permeabilized in 0.5% Triton-100 for 10–15 min, and then washed in 1X PBS. Primary antibody was cultured in 1% BSA 1X PBS overnight at 4°C, and then washed in 1X PBS. Secondary antibody was cultured in 1X PBS for 1–2 h at room temperature, and then washed in 1X PBS. Cells were filtered before run flow cytometry.

Teratoma experiment. The teratoma formation experiment was approved by the Animal Ethics Committee of the University of Macau. Male nude mice at ages of 6–7 weeks were used for teratoma test, with 3 mice for each treatment. hPSCs were cultured in E8 medium with treatment for 70%–80% cell density in 6-well plate before harvesting. Cells were dissociated by EDTA condition and suspended in 200 μL Matrigel mixture (E8: Matrigel to 2:1 mixture with 1:1000 Y27632). Cells were injected to hindlimb intramuscular. After cell injection, the tumor was removed after 6–8 weeks. Tumor was cut to small slices and put in 50 mL tube with 4% PFA overnight in 4°C. Tissue processor and paraffin embedding were processed after fixing. After slicing and H&E staining, three germ layers (mesoderm, endoderm, and ectoderm) of teratoma were analyzed on NDP view software.

Generation of MAPK7 *(*ERK5*) knockdown cell line*. sh*MAPK7* primers were designed on the website (http://rnaidesigner.thermofisher.com/rnaiexpress/). sh*MAPK7* primers were annealed and ligated in to pLKO.1 vector. Lentiviral sh*MAPK7* was generated in 293FT cells. sh*MAPK7* H1 ESC cell line was established after Lentiviral sh*MAPK7* transduced in H1 ESCs and selected by puromycin (Fisher Scientific). sh*MAPK7* primers were listed in the Table S2.

Generation of MAP2K5DD *(*MEK5DD*) overexpression cell line*. *MAP2K5DD* mutation (changed Ser311 to Asp, Ser315 to Asp) sequence was subcloned into EZ-Lv195.1 cloning vector (iGenebio). Lentiviral *MAP2K5DD* was generated in 293FT cells. MAP2K5DD-OE H1 ESC cell line was established after Lentiviral *MAP2K5DD* transduced in H1 ESCs and selected by puromycin (Fisher Scientific).

RNA-seq and data analysis. Cells were harvested in RNAiso Plus reagent (Takara). The poly(A) mRNA isolation was performed using Oligo(dT) beads according to manufacturer's instructions. 1 μg total RNA was used for following library preparation. The RNA library was sequenced for paired end reads on Illumina NextSeq 500 (Illumina).

Quality control of RNA-seq raw data was performed using Trimmomatic version 0.36 (Bolger et al., 2014) (ILLUMINACLIP: TruSeq3-PE.fa:2:30:10:8:true SLIDINGWINDOW:4:15 LEADING:3 TRAILING:3 MINLEN:50). RNA-seq clean data alignment was conducted using STAR version 020201 (Dobin et al., 2013) with the reference genome hg38. All gene expressions were quantified using

FeatureCounts version 1.5.3 (Liao et al., 2014). Differentially expressed genes (DEGs) were identified with the criteria of p adjusted value <0.05 and the absolute value of log2(fold change) >1 after profile normalized using DESeq2 version 1.26.0 (Love et al., 2014).

DEG analysis was performed using the GO and KEGG enrichment analysis through the R package ClusterProfiler 4.0 (Wu et al., 2021).

Re-analysis of public RNA-seq of hiPSCs. Raw counts of RNA-seq data of 317 hiPSC lines were downloaded from publication (Carcamo-Orive et al., 2022) (GSE79636). Count data were processed as single cells using the Seurat package version 4.1.0 (Hao et al., 2021). The raw counts were normalized using LogNormalize method with 1,000,000 as the scale factor. FindVariableFeatures function was used to identify the top 2,000 variable features. Then RunUMAP function was used to perform UMAP on the top 30 principal components for visualizing the cells.

Statistical analysis. Data were presented as mean ± SD of three independent experiments. p values were calculated using one-way ANOVA test, $*p < 0.05$, ns, not significant.

SUPPLEMENTAL INFORMATION

Supplemental information can be found online at https://doi.org/10.1016/j.stemcr.2024.07.007.

ACKNOWLEDGMENTS

This project was funded by University of Macau (file no. MYRG2018-00135-FHS, MYRG2019-00147-FHS, and MYRG-GRG2023-00137-FHS-UMDF), the Science and Technology Development Fund, Macau SAR (file no. 0059/2019/A1, 0123/2019/A3, 0002/2021/AKP, 0085/2023/AMJ, 0002/2023/RIB1, 0010/2023/AKP, and 0073/2023/ITP2), and MOST Key R&D grant (file no. 2022YFA1105000). We would like to thank the Biological Imaging and Stem Cell Core and the Animal Research Core at the Faculty of Health Sciences, University of Macau for their technical support.

AUTHOR CONTRIBUTIONS

G.C. and C.S. designed the project. C.S. and X.W. conducted cell culture experiments and processed RT-qPCR and western blotting test. C.S., D.L., and Z.H. conducted RNA-seq and ChIP-seq data processing and data analysis. C.S. and Z.Z. conducted teratoma experiment and tissue histopathology processing. C.S., W.L., and G.C. wrote the manuscript. Most authors contributed effort to the editing of the manuscript.

DECLARATION OF INTERESTS

C.S. and G.C. filed a patent application based on early lineage-specific differentiation and cardiomyocyte differentiation that is induced by ERK5 inhibitor.

Received: November 28, 2023
Revised: July 21, 2024
Accepted: July 22, 2024
Published: August 15, 2024

REFERENCES

Battle, S.L., Doni Jayavelu, N., Azad, R.N., Hesson, J., Ahmed, F.N., Overbey, E.G., Zoller, J.A., Mathieu, J., Ruohola-Baker, H., Ware, C.B., and Hawkins, R.D. (2019). Enhancer Chromatin and 3D Genome Architecture Changes from Naive to Primed Human Embryonic Stem Cell States. Stem Cell Rep. *12*, 1129–1144.

Beers, J., Gulbranson, D.R., George, N., Siniscalchi, L.I., Jones, J., Thomson, J.A., and Chen, G. (2012). Passaging and colony expansion of human pluripotent stem cells by enzyme-free dissociation in chemically defined culture conditions. Nat. Protoc. *7*, 2029–2040.

Bernardo, A.S., Faial, T., Gardner, L., Niakan, K.K., Ortmann, D., Senner, C.E., Callery, E.M., Trotter, M.W., Hemberger, M., Smith, J.C., et al. (2011). BRACHYURY and CDX2 mediate BMP-induced differentiation of human and mouse pluripotent stem cells into embryonic and extraembryonic lineages. Cell Stem Cell *9*, 144–155.

Bolger, A.M., Lohse, M., and Usadel, B. (2014). Trimmomatic: a flexible trimmer for Illumina sequence data. Bioinformatics *30*, 2114–2120.

Brown, H.A., Williams, C.A.C., Zhou, H., Rios-Szwed, D., Fernandez-Alonso, R., Mansoor, S., McMulkin, L., Toth, R., Gourlay, R., Peltier, J., et al. (2021). An ERK5-KLF2 signalling module regulates early embryonic gene expression and telomere rejuvenation in stem cells. Biochem. J. *478*, 4119–4136.

Burrows, C.K., Banovich, N.E., Pavlovic, B.J., Patterson, K., Gallego Romero, I., Pritchard, J.K., and Gilad, Y. (2016). Genetic Variation, Not Cell Type of Origin, Underlies the Majority of Identifiable Regulatory Differences in iPSCs. PLoS Genet. *12*, e1005793.

Carcamo-Orive, I., Hoffman, G.E., Cundiff, P., Beckmann, N.D., D'Souza, S.L., Knowles, J.W., Patel, A., Hendry, C., Papatsenko, D., Abbasi, F., et al. (2022). Analysis of Transcriptional Variability in a Large Human iPSC Library Reveals Genetic and Non-genetic Determinants of Heterogeneity. Cell Stem Cell *29*, 1505.

Carcamo-Orive, I., Hoffman, G.E., Cundiff, P., Beckmann, N.D., D'Souza, S.L., Knowles, J.W., Patel, A., Papatsenko, D., Abbasi, F., Reaven, G.M., et al. (2017). Analysis of Transcriptional Variability in a Large Human iPSC Library Reveals Genetic and Non-genetic Determinants of Heterogeneity. Cell Stem Cell *20*, 518–532.e9.

Chambers, S.M., Fasano, C.A., Papapetrou, E.P., Tomishima, M., Sadelain, M., and Studer, L. (2009). Highly efficient neural conversion of human ES and iPS cells by dual inhibition of SMAD signaling. Nat. Biotechnol. *27*, 275–280.

Chen, G., Gulbranson, D.R., Hou, Z., Bolin, J.M., Ruotti, V., Probasco, M.D., Smuga-Otto, K., Howden, S.E., Diol, N.R., Propson, N.E., et al. (2011). Chemically defined conditions for human iPSC derivation and culture. Nat. Methods *8*, 424–429.

Cliff, T.S., Wu, T., Boward, B.R., Yin, A., Yin, H., Glushka, J.N., Prestegaard, J.H., and Dalton, S. (2017). MYC Controls Human Pluripotent Stem Cell Fate Decisions through Regulation of Metabolic Flux. Cell Stem Cell *21*, 502–516.e9.

Creyghton, M.P., Cheng, A.W., Welstead, G.G., Kooistra, T., Carey, B.W., Steine, E.J., Hanna, J., Lodato, M.A., Frampton, G.M., Sharp, P.A., et al. (2010). Histone H3K27ac separates active from poised

enhancers and predicts developmental state. Proc. Natl. Acad. Sci. USA *107*, 21931–21936.

Deng, C., Zhang, Z., Xu, F., Xu, J., Ren, Z., Godoy-Parejo, C., Xiao, X., Liu, W., Zhou, Z., and Chen, G. (2022). Thyroid hormone enhances stem cell maintenance and promotes lineage-specific differentiation in human embryonic stem cells. Stem Cell Res. Ther. *13*, 120.

Dobin, A., Davis, C.A., Schlesinger, F., Drenkow, J., Zaleski, C., Jha, S., Batut, P., Chaisson, M., and Gingeras, T.R. (2013). STAR: ultrafast universal RNA-seq aligner. Bioinformatics *29*, 15–21.

Drew, B.A., Burow, M.E., and Beckman, B.S. (2012). MEK5/ERK5 pathway: the first fifteen years. Biochim. Biophys. Acta *1825*, 37–48.

English, J.M., Pearson, G., Baer, R., and Cobb, M.H. (1998). Identification of substrates and regulators of the mitogen-activated protein kinase ERK5 using chimeric protein kinases. J. Biol. Chem. *273*, 3854–3860.

English, J.M., Pearson, G., Hockenberry, T., Shivakumar, L., White, M.A., and Cobb, M.H. (1999). Contribution of the ERK5/MEK5 pathway to Ras/Raf signaling and growth control. J. Biol. Chem. *274*, 31588–31592.

Gatchalian, J., Malik, S., Ho, J., Lee, D.S., Kelso, T.W.R., Shokhirev, M.N., Dixon, J.R., and Hargreaves, D.C. (2018). A non-canonical BRD9-containing BAF chromatin remodeling complex regulates naive pluripotency in mouse embryonic stem cells. Nat. Commun. *9*, 5139.

Godoy-Parejo, C., Deng, C., Liu, W., and Chen, G. (2019). Insulin Stimulates PI3K/AKT and Cell Adhesion to Promote the Survival of Individualized Human Embryonic Stem Cells. Stem Cell. *37*, 1030–1041.

Greber, B. (2011). When BMP meets FGF. Cell Stem Cell *9*, 91–92.

Gu, W., Gaeta, X., Sahakyan, A., Chan, A.B., Hong, C.S., Kim, R., Braas, D., Plath, K., Lowry, W.E., and Christofk, H.R. (2016). Glycolytic Metabolism Plays a Functional Role in Regulating Human Pluripotent Stem Cell State. Cell Stem Cell *19*, 476–490.

Hao, Y., Hao, S., Andersen-Nissen, E., Mauck, W.M., 3rd, Zheng, S., Butler, A., Lee, M.J., Wilk, A.J., Darby, C., Zager, M., et al. (2021). Integrated analysis of multimodal single-cell data. Cell *184*, 3573–3587.e29.

Hawkins, R.D., Hon, G.C., Lee, L.K., Ngo, Q., Lister, R., Pelizzola, M., Edsall, L.E., Kuan, S., Luu, Y., Klugman, S., et al. (2010). Distinct Epigenomic Landscapes of Pluripotent and Lineage-Committed Human Cells. Cell Stem Cell *6*, 479–491.

Kato, Y., Kravchenko, V.V., Tapping, R.I., Han, J., Ulevitch, R.J., and Lee, J.D. (1997). BMK1/ERK5 regulates serum-induced early gene expression through transcription factor MEF2C. Embo Journal *16*, 7054–7066.

Li, L., Song, L., Liu, C., Chen, J., Peng, G., Wang, R., Liu, P., Tang, K., Rossant, J., and Jing, N. (2015). Ectodermal progenitors derived from epiblast stem cells by inhibition of Nodal signaling. J. Mol. Cell Biol. *7*, 455–465.

Liang, C.J., Wang, Z.W., Chang, Y.W., Lee, K.C., Lin, W.H., and Lee, J.L. (2019). SFRPs Are Biphasic Modulators of Wnt-Signaling-Elicited Cancer Stem Cell Properties beyond Extracellular Control. Cell Rep. *28*, 1511–1525.e5.

Liao, Y., Smyth, G.K., and Shi, W. (2014). featureCounts: an efficient general purpose program for assigning sequence reads to genomic features. Bioinformatics *30*, 923–930.

Lindsley, R.C., Gill, J.G., Kyba, M., Murphy, T.L., and Murphy, K.M. (2006). Canonical Wnt signaling is required for development of embryonic stem cell-derived mesoderm. Development *133*, 3787–3796.

Liu, L., Nemashkalo, A., Rezende, L., Jung, J.Y., Chhabra, S., Guerra, M.C., Heemskerk, I., and Warmflash, A. (2022). Nodal is a short-range morphogen with activity that spreads through a relay mechanism in human gastruloids. Nat. Commun. *13*, 497.

Love, M.I., Huber, W., and Anders, S. (2014). Moderated estimation of fold change and dispersion for RNA-seq data with DESeq2. Genome Biol. *15*, 550.

Madhu, V., Dighe, A.S., Cui, Q., and Deal, D.N. (2016). Dual Inhibition of Activin/Nodal/TGF-beta and BMP Signaling Pathways by SB431542 and Dorsomorphin Induces Neuronal Differentiation of Human Adipose Derived Stem Cells. Stem Cell. Int. *2016*, 1035374.

Morikawa, M., Koinuma, D., Mizutani, A., Kawasaki, N., Holmborn, K., Sundqvist, A., Tsutsumi, S., Watabe, T., Aburatani, H., Heldin, C.H., and Miyazono, K. (2016). BMP Sustains Embryonic Stem Cell Self-Renewal through Distinct Functions of Different Kruppel-like Factors. Stem Cell Rep. *6*, 64–73.

Nithianandarajah-Jones, G.N., Wilm, B., Goldring, C.E.P., Müller, J., and Cross, M.J. (2012). ERK5: structure, regulation and function. Cell. Signal. *24*, 2187–2196.

Pan, G., Tian, S., Nie, J., Yang, C., Ruotti, V., Wei, H., Jonsdottir, G.A., Stewart, R., and Thomson, J.A. (2007). Whole-genome analysis of histone H3 lysine 4 and lysine 27 methylation in human embryonic stem cells. Cell Stem Cell *1*, 299–312.

Paudel, R., Fusi, L., and Schmidt, M. (2021). The MEK5/ERK5 Pathway in Health and Disease. Int. J. Mol. Sci. *22*, 7594.

Pera, M.F., and Rossant, J. (2021). The exploration of pluripotency space: Charting cell state transitions in peri-implantation development. Cell Stem Cell *28*, 1896–1906.

Ren, Z., Zhong, H., Song, C., Deng, C., Hsieh, H.T., Liu, W., and Chen, G. (2020). Insulin Promotes Mitochondrial Respiration and Survival through PI3K/AKT/GSK3 Pathway in Human Embryonic Stem Cells. Stem Cell Rep. *15*, 1362–1376.

Rouhani, F., Kumasaka, N., de Brito, M.C., Bradley, A., Vallier, L., and Gaffney, D. (2014). Genetic background drives transcriptional variation in human induced pluripotent stem cells. PLoS Genet. *10*, e1004432.

Song, C., Xu, F., Ren, Z., Zhang, Y., Meng, Y., Yang, Y., Lingadahalli, S., Cheung, E., Li, G., Liu, W., et al. (2019). Elevated Exogenous Pyruvate Potentiates Mesodermal Differentiation through Metabolic Modulation and AMPK/mTOR Pathway in Human Embryonic Stem Cells. Stem Cell Rep. *13*, 338–351.

Stecca, B., and Rovida, E. (2019). Impact of ERK5 on the Hallmarks of Cancer. Int. J. Mol. Sci. *20*, 1426.

Sunadome, K., Yamamoto, T., Ebisuya, M., Kondoh, K., Sehara-Fujisawa, A., and Nishida, E. (2011). ERK5 regulates muscle cell fusion through Klf transcription factors. Dev. Cell *20*, 192–205.

Takahashi, K., and Yamanaka, S. (2006). Induction of pluripotent stem cells from mouse embryonic and adult fibroblast cultures by defined factors. Cell *126*, 663–676.

Thakurela, S., Tiwari, N., Schick, S., Garding, A., Ivanek, R., Berninger, B., and Tiwari, V.K. (2016). Mapping gene regulatory circuitry of Pax6 during neurogenesis. Cell Discov. *2*, 15045.

Thomson, J.A., Itskovitz-Eldor, J., Shapiro, S.S., Waknitz, M.A., Swiergiel, J.J., Marshall, V.S., and Jones, J.M. (1998). Embryonic stem cell lines derived from human blastocysts. Science *282*, 1145–1147.

Uren, A., Reichsman, F., Anest, V., Taylor, W.G., Muraiso, K., Bottaro, D.P., Cumberledge, S., and Rubin, J.S. (2000). Secreted frizzled-related protein-1 binds directly to wingless and is a biphasic modulator of Wnt signaling. J. Biol. Chem. *275*, 4374–4382.

Watanabe, M., Buth, J.E., Haney, J.R., Vishlaghi, N., Turcios, F., Elahi, L.S., Gu, W., Pearson, C.A., Kurdian, A., Baliaouri, N.V., et al. (2022). TGFb superfamily signaling regulates the state of human stem cell pluripotency and capacity to create well-structured telencephalic organoids. Stem Cell Rep. *17*, 2220–2238.

Wattanapanitch, M., Klincumhom, N., Potirat, P., Amornpisutt, R., Lorthongpanich, C., U-pratya, Y., Laowtammathron, C., Kheolamai, P., Poungvarin, N., and Issaragrisil, S. (2014). Dual small-molecule targeting of SMAD signaling stimulates human induced pluripotent stem cells toward neural lineages. PLoS One *9*, e106952.

Williams, C.A.C., Fernandez-Alonso, R., Wang, J., Toth, R., Gray, N.S., and Findlay, G.M. (2016). Erk5 Is a Key Regulator of Naive-Primed Transition and Embryonic Stem Cell Identity. Cell Rep. *16*, 1820–1828.

Wu, T., Hu, E., Xu, S., Chen, M., Guo, P., Dai, Z., Feng, T., Zhou, L., Tang, W., Zhan, L., et al. (2021). clusterProfiler 4.0: A universal enrichment tool for interpreting omics data. Innovation *2*, 100141.

Xu, F., Deng, C., Ren, Z., Sun, L., Meng, Y., Liu, W., Wan, J., and Chen, G. (2021). Lysophosphatidic acid shifts metabolic and transcriptional landscapes to induce a distinct cellular state in human pluripotent stem cells. Cell Rep. *37*, 110063.

Xu, R.H., Chen, X., Li, D.S., Li, R., Addicks, G.C., Glennon, C., Zwaka, T.P., and Thomson, J.A. (2002). BMP4 initiates human embryonic stem cell differentiation to trophoblast. Nat. Biotechnol. *20*, 1261–1264.

Yan, L., Carr, J., Ashby, P.R., Murry-Tait, V., Thompson, C., and Arthur, J.S.C. (2003). Knockout of ERK5 causes multiple defects in placental and embryonic development. BMC Dev. Biol. *3*, 11.

Yu, J., Vodyanik, M.A., Smuga-Otto, K., Antosiewicz-Bourget, J., Frane, J.L., Tian, S., Nie, J., Jonsdottir, G.A., Ruotti, V., Stewart, R., et al. (2007). Induced pluripotent stem cell lines derived from human somatic cells. Science *318*, 1917–1920.

Yu, P., Pan, G., Yu, J., and Thomson, J.A. (2011). FGF2 sustains NANOG and switches the outcome of BMP4-induced human embryonic stem cell differentiation. Cell Stem Cell *8*, 326–334.

Zhang, P., Li, J., Tan, Z., Wang, C., Liu, T., Chen, L., Yong, J., Jiang, W., Sun, X., Du, L., et al. (2008). Short-term BMP-4 treatment initiates mesoderm induction in human embryonic stem cells. Blood *111*, 1933–1941.

Zhang, W., Chronis, C., Chen, X., Zhang, H., Spalinskas, R., Pardo, M., Chen, L., Wu, G., Zhu, Z., Yu, Y., et al. (2019). The BAF and PRC2 Complex Subunits Dpf2 and Eed Antagonistically Converge on Tbx3 to Control ESC Differentiation. Cell Stem Cell *24*, 138–152.e8.

Zhong, H., Ren, Z., Wang, X., Miao, K., Ni, W., Meng, Y., Lu, L., Wang, C., Liu, W., Deng, C.X., et al. (2020). Stagewise keratinocyte differentiation from human embryonic stem cells by defined signal transduction modulators. Int. J. Biol. Sci. *16*, 1450–1462.

Zhou, X., Ren, Z., Xu, J., Deng, C., Zhang, Z., Godoy-Parejo, C., Xu, F., Huang, E.C.C., Wang, J., Cai, Z., et al. (2022). Insulin Directs Dichotomous Translational Regulation to Control Human Pluripotent Stem Cell Survival, Proliferation and Pluripotency. Int. J. Biol. Sci. *18*, 3562–3575.